

Supplementary Materials for
**Should we think of observationally constrained multidecade climate
projections as predictions?**

Tong Li *et al.*

Corresponding author: Francis W. Zwiers, fwzwiers@uvic.ca

Sci. Adv. **11**, eadt6485 (2025)
DOI: 10.1126/sciadv.adt6485

This PDF file includes:

Figs. S1 to S8
Table S1

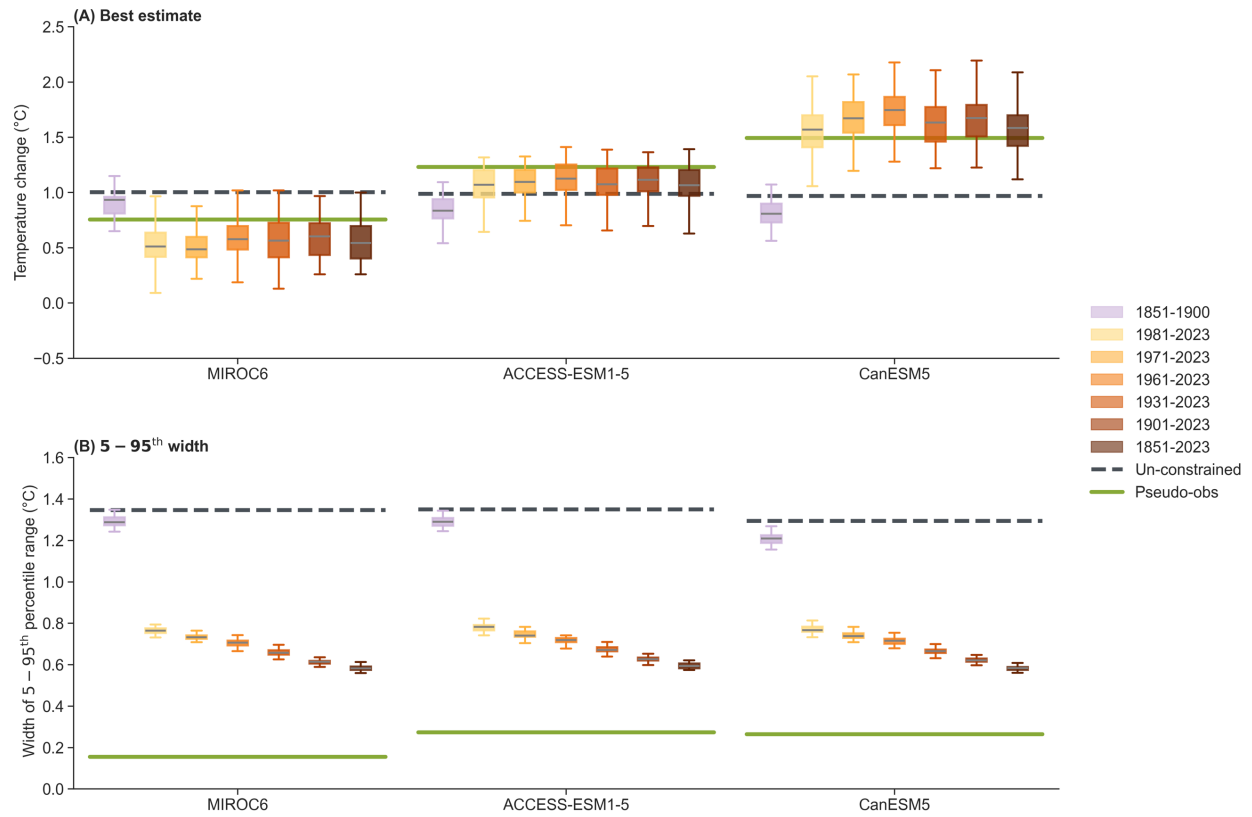


Fig. S1. Observational constraints with the KCC method can effectively reduce bias and model uncertainty in multi-model projections. Same as **Fig. 1** but for SSP1-2.6 emissions scenario.

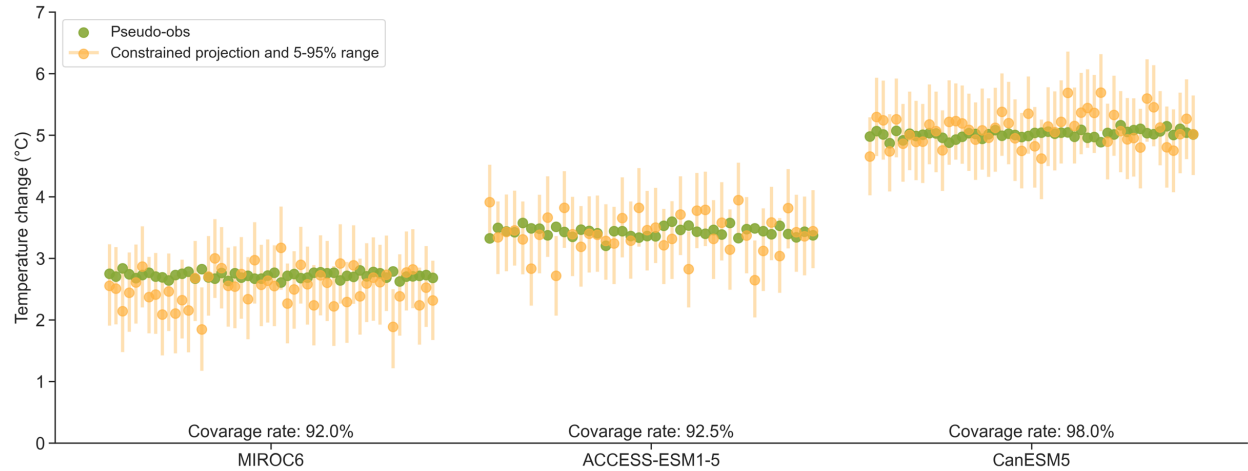


Fig. S2. Almost all predictions from a given large ensemble fall within the 5-95% uncertainty range of the constrained projection. Projected changes in global mean temperature from pseudo-observations (individual runs of a large ensemble, green dots) and the corresponding constrained projections based on a 1901-2023 constraint period (constrained projections based on individual runs of large ensemble, orange dots), associated with 5-95% confidence intervals (error bar) for the future 20-year period (2074-2093) at a 50-year lead time relative to current climate condition (1994-2023) (Unit: °C).

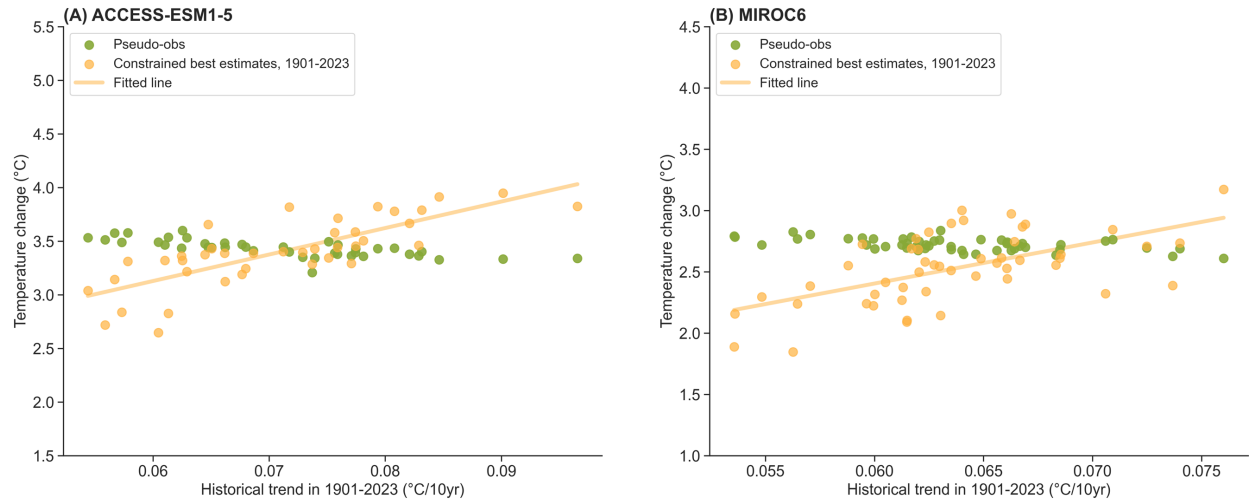


Fig. S3. Natural variability in the observation can affect observation-constrained projections. Same as **Fig. 2** but for pseudo-observation simulated by (A) ACCESS-E SM1-5 and (B) MIROC6.



Fig. S4. Comparison using different constraint approaches and varying lengths of pseudo-observational records from the mid-sensitivity model ACCESS-ESM1-5. Same as **Fig. 3**, but for pseudo-observations simulated by ACCESS-ESM1-5. Note that the results constrained by the full time series are identical to those in **Fig. 1** for pseudo-observations from ACCESS-ESM1-5.



Fig. S5. Comparison using different constraint approaches and varying lengths of pseudo-observational records from the low-sensitivity model MIROC6. Same as **Fig. 3**, but for pseudo-observations simulated by MIROC6. Note that the results constrained by the full time series are identical to those in **Fig. 1** for pseudo-observations from MIROC6.

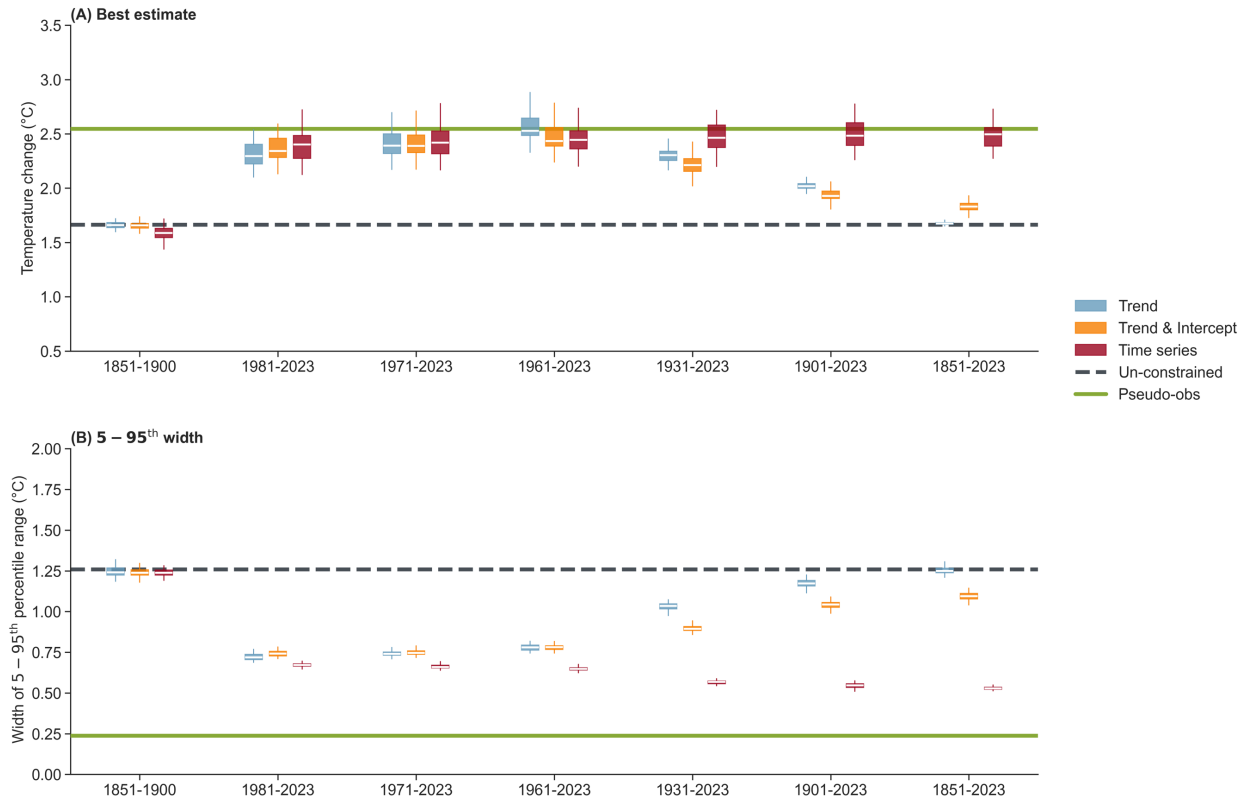


Fig. S6. Comparison using different constraint approaches and varying lengths of pseudo-observational records for a shorter 20-year lead time. Same as Fig. 3, but for a 20-year lead time.

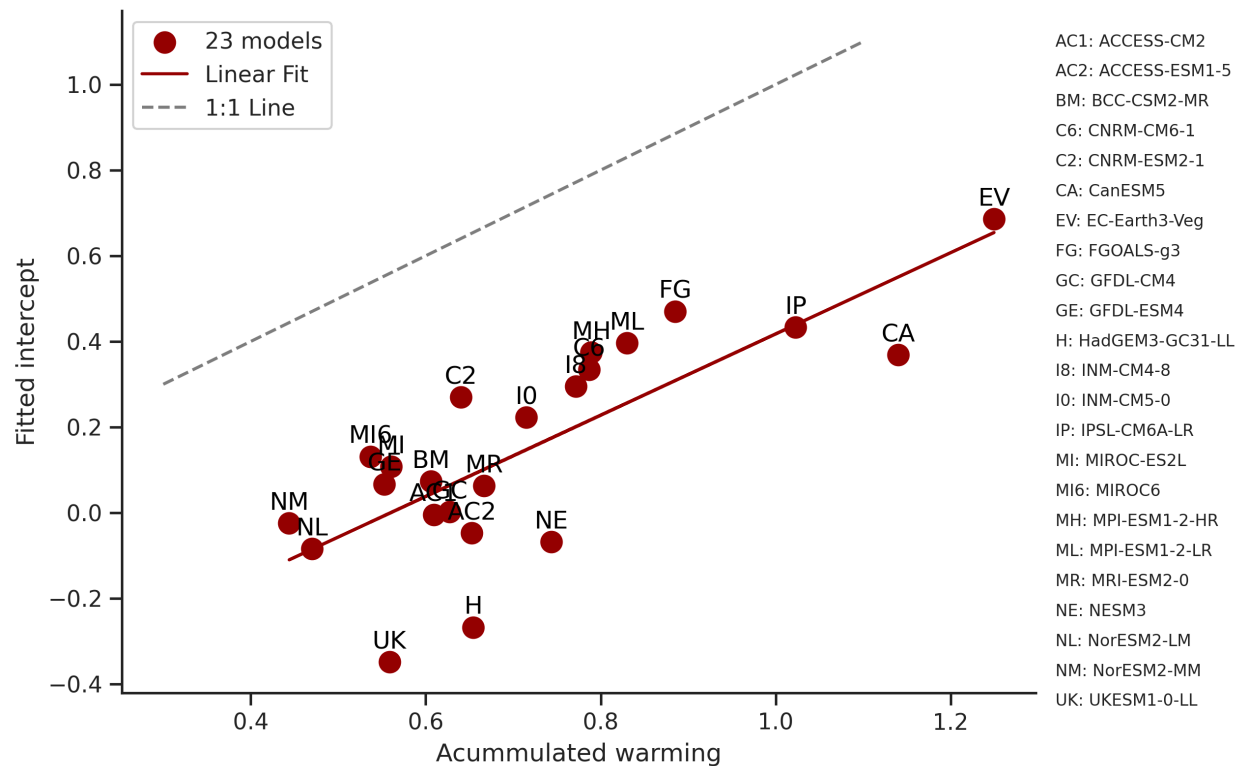


Fig. S7. Relationship between the intercepts of the linear trends fitted to the 1981-2023

series and the warming by 1981 relative to pre-industrial levels in CMIP6 models. The slope of the linear trend can be interpreted as providing information about the rate at which the surface climate warms after warming during the constraint period, when warming is well underway, while the intercept gives information about the warming that occurred prior to the constraint period. Models where surface temperature begins to warm more quickly after the start of the industrial period will show greater warming between preindustrial and the constraint period.

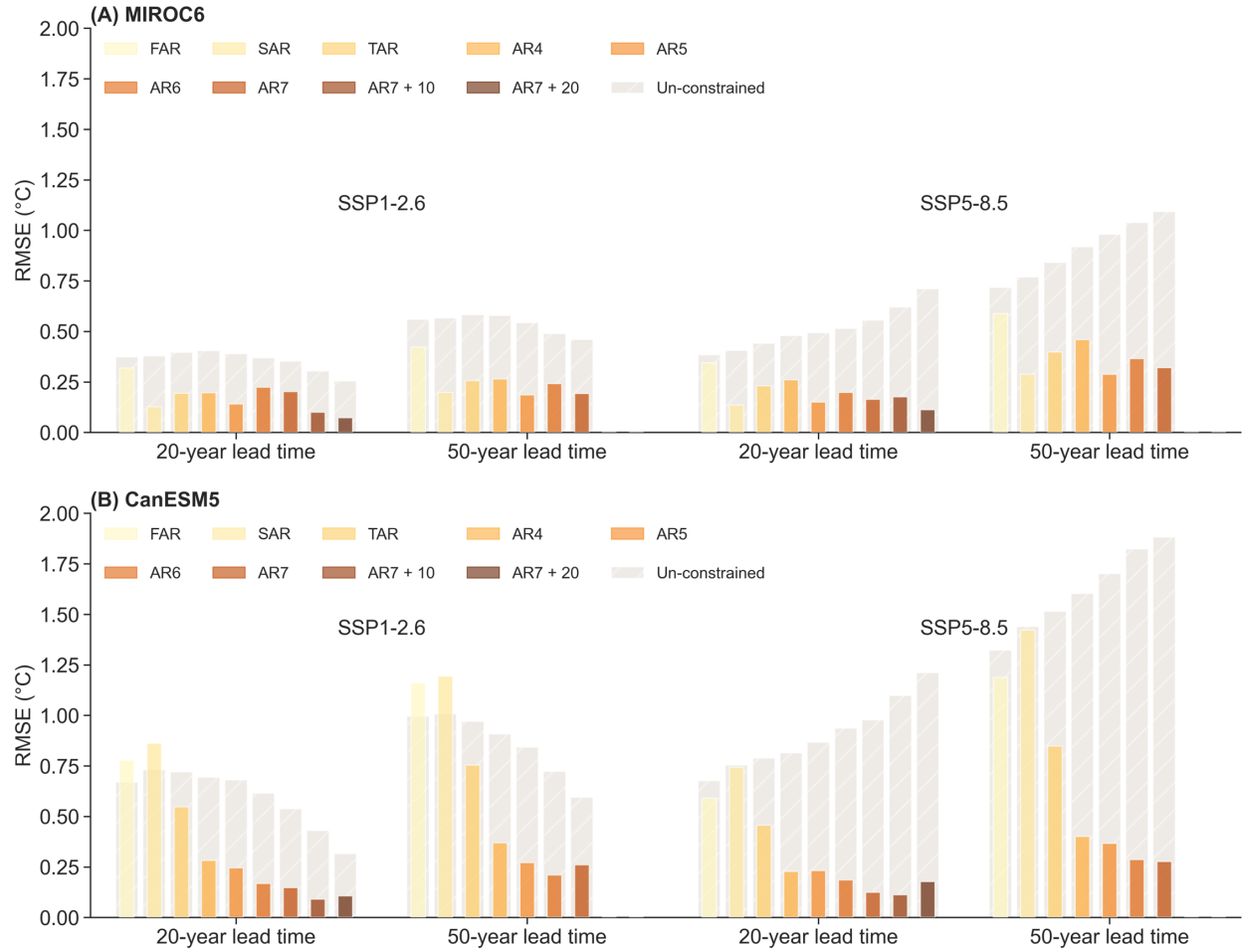


Fig. S8. Predictive skill when using pseudo-observations from the low-sensitivity model MIROC6 and high-sensitivity model CanESM5. Same as Fig. 5 (A) but for pseudo-observations simulated by (A) MIROC6 and (B) CanESM5.

Table S1. A list of the models whose simulations are used in this study and corresponding number of realizations. The models that produced the large ensembles used as pseudo-observations in the imperfect model testing procedure are indicated in bold, and the 16 models used in the estimation of internal variability are indicated in italics.

Model Experiment					Model Experiment				
		Historical	SSP 1-2.6	SSP 5-8.5			Historical	SSP 1-2.6	SSP 5-8.5
1	<i>ACCESS-CM2</i>	3	10	3	13	<i>INM-CM5-0</i>	1	1	1
2	<i>ACCESS-ESM1-5</i>	40	40	40	14	<i>IPSL-CM6A-LR</i>	32	6	6
3	<i>BCC-CSM2-MR</i>	3	1	1	15	<i>MIROC-ES2L</i>	30	10	10
4	<i>CNRM-CM6-1</i>	6	6	6	16	<i>MIROC6</i>	50	50	50
5	<i>CNRM-ESM2-1</i>	5	5	4	17	<i>MPI-ESM1-2-HR</i>	10	2	2
6	<i>CanESM5</i>	50	50	50	18	<i>MPI-ESM1-2-LR</i>	10	40	40
7	<i>EC-Earth-Veg</i>	9		8	19	<i>MRI-ESM2-0</i>	10	5	5
8	<i>FGOALS-g3</i>	4	3	3	20	<i>NESM3</i>	5	2	2
9	<i>GFDL-CM4</i>	1		1	21	<i>NorESM2-LM</i>	3	1	1
10	<i>GFDL-ESM4</i>	3	1	1	22	<i>NorESM2-MM</i>	2	1	1
11	<i>HadGEM3-GC31-LL</i>	5	1	4	23	<i>UKESM1-0-LL</i>	19	19	5
12	<i>INM-CM4-8</i>	1	1	1					